Tsuda *et al. Earth, Planets and Space* (2019) 71:109
https://doi.org/10.1186/s40623-019-1091-x

Earth, Planets and Space

EXPRESS LETTER

Open Access

Origin of the seismic belt in the San-in district, southwest Japan, inferred from the seismic velocity structure of the lower crust

Hiroo Tsuda[1*], Yoshihisa Iio[2] and Takuo Shibutani[2]

Abstract

A long linear distribution of epicenters is seen along the Japan Sea coast in the San-in district located in southwestern Japan. This linear distribution of epicenters is called the seismic belt in the San-in district. The localization of intraplate earthquakes in the San-in district, far from plate boundaries, is not well understood. To answer this question, we look at the seismic velocity structure of the lower crust beneath the San-in district using seismic travel-time tomography. Our results show the existence of a low-velocity anomaly in the lower crust beneath the seismic belt. We infer that the deformation was concentrated in the low-velocity zone due to compressive stress caused by the subduction of oceanic plates, that stress concentration occurred just above the low-velocity zone, and that the seismic belt was therefore formed there. We also calculated the cutoff depths of shallow intraplate earthquakes in the San-in district. Based on the results, we consider the possible causes of the low-velocity anomaly in the lower crust beneath the seismic belt. We found that the cutoff depths of the intraplate earthquakes were shallower in the eastern part of the low-velocity zone in the lower crust beneath the seismic belt and deeper in the western part. Thus, the eastern part is likely to be hotter than the western part. We inferred that the eastern part was hot because a hot mantle upwelling approaches the Moho discontinuity below it and the resulting high temperature may be the main cause of the low-velocity anomaly. On the other hand, in the western part, we inferred that the temperature is not high because the mantle upwelling may not exist at shallow depth, and water dehydrated from the Philippine Sea plate reaches the lower crust, and the existence of this water may be the main cause of the low-velocity anomaly.

Keywords: Seismic belt, San-in district, Travel-time tomography, Lower crust, Low-velocity zone, Cutoff depth of earthquakes

Introduction

A long linear distribution of epicenters is seen along the Japan Sea coast in the San-in district, located in southwestern Japan (Nakao et al. 1991). The linear distribution of epicenters is called the seismic belt in the San-in district. The epicenters of intraplate earthquakes of M_J (Japan Meteorological Agency magnitude) ≥ 1.0 and depths ≤ 20 km that occurred between January 2001 and December 2016 are plotted in Fig. 1a, along with the epicenters of large intraplate earthquakes of $M_J \geq 6.5$ that have occurred over the past 100 years. Large intraplate earthquakes occurred in the seismic belt in 1943 ($M_J = 7.2$), 1997 ($M_J = 6.6$), 2000 ($M_J = 7.3$), and 2016 ($M_J = 6.6$).

Southwestern Japan is considered to be located in the Amur plate, which is a continental plate (e.g., Heki et al. 1999) (Fig. 1b). The increasing of strain in the Amur plate as a result of the subduction of the Philippine Sea (PHS) plate from the southeast and the Pacific (PAC) plate from the east leads to the occurrence of intraplate earthquakes in southwestern Japan. Kawanishi et al. (2009), who conducted stress inversions in the San-in district, noted that

*Correspondence: tsuda.hiroo.87x@st.kyoto-u.ac.jp
[1] Graduate School of Science, Kyoto University, Kyoto, Japan
Full list of author information is available at the end of the article

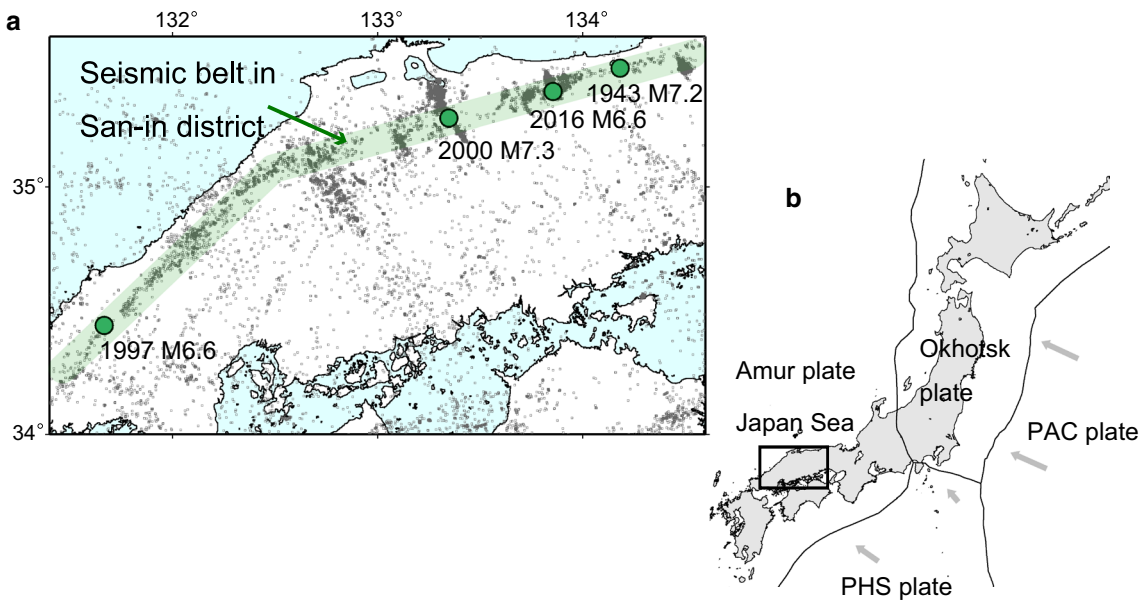

Fig. 1 **a** The seismic belt in the San-in district. Gray dots denote epicenters of intraplate earthquakes of $M_J \geq 1.0$ and depths ≤ 20 km that occurred between January 2001 and December 2016. Green circles denote epicenters of large intraplate earthquakes of $M_J \geq 6.5$ that occurred over the past 100 years. **b** Tectonic setting in and around the Japanese Islands. The rectangle outlines the area shown in **a**. Gray arrows indicate the plate motion of the oceanic plates relative to the continental plates

stress concentrations occur in the San-in district and that occurrences of intraplate earthquakes were localized in the seismic belt. Nishimura and Takada (2017) analyzed GNSS data and found that the strain rate was high in the San-in district. However, reasons why the stress and strain rate are concentrated in the San-in district, far from the plate boundaries, and why intraplate earthquakes are localized there are not well understood. To answer these questions, we examined the process by which intraplate earthquakes are generated.

Iio et al. (2002) proposed a model of the process by which intraplate earthquakes are generated. In their model, the presence of a low-viscosity zone in the lower continental crust could control the localization of intraplate earthquakes. We call the low-viscosity zone in the lower crust the "weak zone". The origin of the seismic belt in the San-in district can be explained by this model. There is the weak zone in the lower crust beneath the seismic belt, and the deformation is concentrated in the weak zone by compressive stress caused by subductions of the PHS plate and the PAC plate, and stress concentration occurs above the weak zone, and many intraplate earthquakes occur there as a result. Kawanishi et al. (2009) and Nishimura and Takada (2017) reproduced stress and strain rate concentrations in the San-in district using model calculations in which they assumed that there was a low-viscosity zone or an aseismic fault in the lower crust beneath the seismic belt. However, they did not prove the existence of such a weak zone in the lower crust beneath the seismic belt. Therefore, to clarify the origin of this seismic belt, we studied whether the lower crust beneath the seismic belt is the weak zone, that is, whether or not it is a low-viscosity zone.

It is known that in a ductile regime, the viscosity of rock is low at high temperatures or high water contents (e.g., Kohlstedt et al. 1995). It is also known that seismic wave velocities in rock are low at high temperatures (e.g., Christensen 1979) or high fluid contents (e.g., O'Connell and Budiansky 1974). Accordingly, low-velocity rock is likely to have lower viscosity. Therefore, to verify that the viscosity of the lower crust beneath the seismic belt is low, we examined whether the lower crust could be characterized as a low-velocity region using seismic travel-time tomography.

Some studies have estimated the seismic velocity structure in the lower crust beneath the San-in district (Zhao et al. 2004, 2018; Nakajima and Hasegawa 2007a, c). Nakajima and Hasegawa (2007a, c) examined the velocity structure throughout the San-in district but focused on the velocity structure in the upper mantle. In this study, we focus on the velocity structure in the lower crust.

Data and method

We estimated the velocity structure in the lower crust beneath the seismic belt using seismic travel-time tomography. For our model space, we set the latitude range to

33°–36°N, the longitude range to 131°–136°E, and the depth range down to 81 km. We used 13,657 earthquakes of $M_J \geq 2.0$ that occurred in the study area between January 2001 and December 2016 (Fig. 2) and the initial locations and origin times of the earthquakes that were determined by the Japan Meteorological Agency (JMA). The P-wave arrival times of these earthquakes were picked at more than 10 stations. We used 368,513 P-wave arrival times of the earthquakes to 291 permanent stations in the study area (Fig. 2), which were picked by the JMA. The earthquakes considered in this study included earthquakes that occurred in the PHS plate (Fig. 2). Seismic rays from earthquakes occurring in the PHS plate at depths of approximately 30–80 km to stations in the San-in district pass through the lower crust beneath the San-in district. Thus, we were able to estimate the velocity structure in the lower crust beneath the seismic belt using the arrival times of these seismic rays.

We used FMTOMO, a tomographic program developed by Rawlinson et al. (2006), to process the data; it can invert wavespeed and source location simultaneously. FMTOMO can trace seismic rays robustly, even if the rays pass through a strong heterogeneous structure, because FMTOMO implements wavefront tracking by the fast marching method (de Kool et al. 2006). FMTOMO is an appropriate tool for the purposes of this study because it makes the robust tracing of rays possible and because the Median Tectonic Line (MTL) and the PHS plate, both of which are characterized by significant velocity anomalies, are located within the study

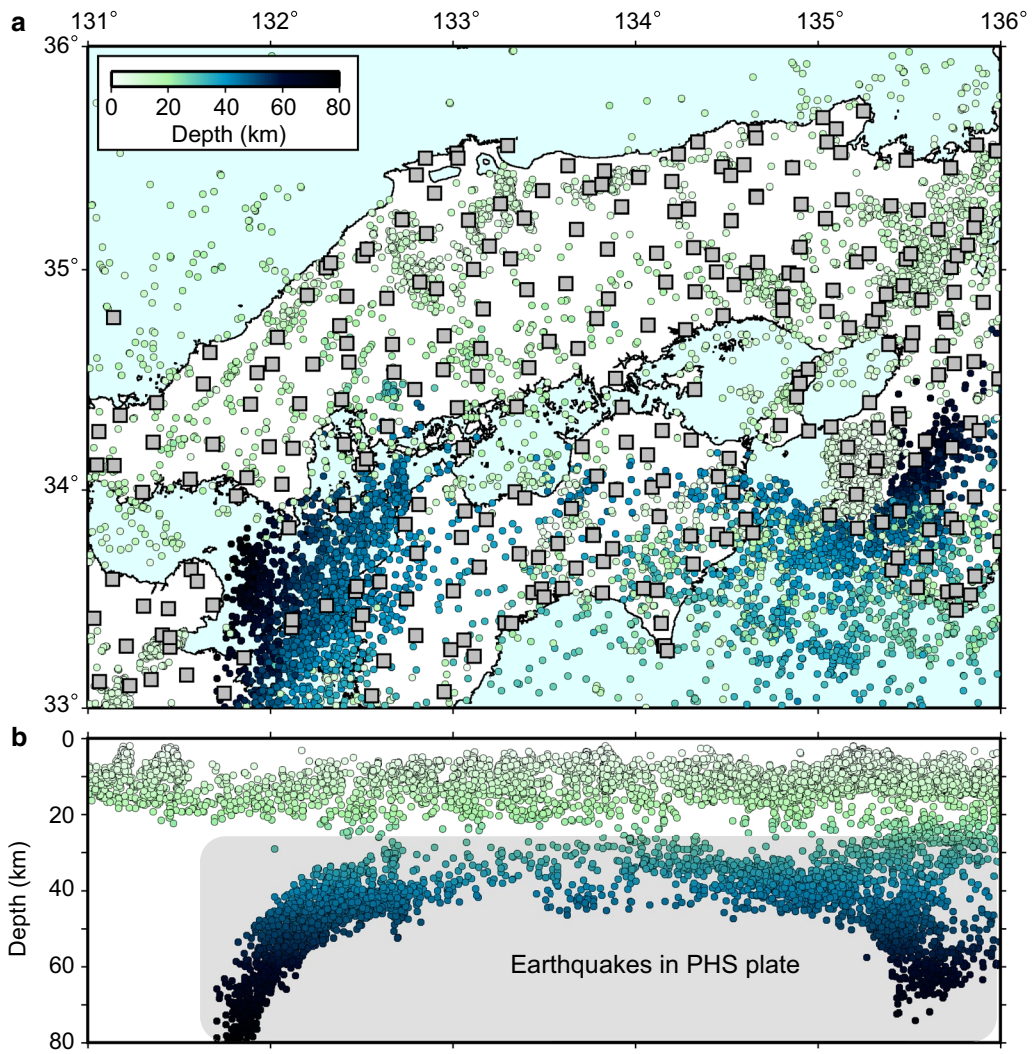

Fig. 2 **a** Distribution of earthquakes (circles) and stations (gray squares) considered in this study. Colors represent the depths of the earthquakes. **b** Depth distribution of the hypocenters projected on vertical cross-section in the east–west direction

area. However, FMTOMO has a drawback in that P- and S-wave velocity structures are not calculated simultaneously. P-wave arrival times are picked more often and more accurately than S-wave arrival times. In particular, it is typically very difficult to pick accurate S-wave arrival times for rays that pass through the PHS plate. Hence, we used only P-wave arrival times in this study.

We set grid nodes with a spacing of 0.1° in the horizontal direction and a spacing of 7 km in the depth direction (4, 11, 18, 25, 32, 39, 46, 53, 60, 67, 74, and 81 km). For the initial model, we used JMA 2001 (Ueno et al. 2002), a 1-D velocity model used in the routine JMA work to determine hypocenter locations. JMA2001 represents the average velocity structure in and around the Japanese islands. We inverted the P-wave velocity (V_P) structure and hypocenter locations. The accuracy of the final hypocenter locations is not considered low because the P-wave arrival times of the earthquakes were picked at more than 10 stations and their epicentral distances were distributed in a wide range and most of these earthquakes occurred inside the seismograph network.

Results and resolution test

Checkerboard resolution test

We carried out a checkerboard resolution test (CRT) to evaluate the reliability of the images obtained. We first developed a checkerboard model by assigning alternating ± 5% velocity perturbations to $3 \times 3 \times 3$ grids of the initial model. We then calculated synthetic arrival times for the checkerboard model. Finally, we added Gaussian random noise with a standard deviation of 0.05 s to the synthetic arrival times, to represent picking errors, and inverted the synthetic data.

The results of the CRT at depths of 4 and 46 km and at 11 and 25 km are shown in Figs. 3b and 4b, respectively. The checkerboard patterns are recovered considerably at depths of 4 and 11 km in inland areas, and that at a depth of 25 km is roughly recovered. Based on the results of the CRT, we have a horizontal resolution of $0.3° \times 0.3°$ in the crust beneath the San-in district. This resolution is high enough to increase the accuracy of estimating heterogeneous structures in the lower crust beneath the seismic belt. The checkerboard pattern in the PHS plate at a depth of 46 km is roughly recovered. Therefore, the reliability of the images obtained for the PHS plate was considered to be high.

Results

The final results were obtained after 10 iterations. The root mean square of the travel-time residuals was reduced from 0.204 s for the initial model to 0.097 s. Figure 3a shows the results of V_P perturbations at depths of 4 and 46 km. V_P perturbations of all the tomographic results (Figs. 3, 4, 5) are deviations from the initial velocity model at each depth. We compared the results with geological structures to evaluate the reliability of the images obtained. At a depth of 4 km, low-velocity anomalies are imaged beneath many quaternary volcanoes. Shibutani et al. (2005) noted the existence of a striking low-velocity anomaly around the Shinji Graben at shallow depths, and our result shows a similar feature. In addition, there are striking velocity anomalies around the MTL. The Ryoke, Chichibu, and Shimanto belts seem to correspond to low-velocity zones, while the Sanbagawa belt seems to correspond to a high-velocity zone. At a depth of 46 km, a high velocity anomaly is imaged in the southern part of the study area (Fig. 3a), which is considered to correspond to the PHS plate. Based on the CRT results and the results of the comparison with the geological structures, such as the quaternary volcanoes, the graben, the MTL, and the PHS plate, the reliability of the images obtained is considered to be high.

Figure 4a shows V_P perturbations at depths of 11 and 25 km, and Fig. 4c shows vertical cross-sections along lines A–C at depths of 0–25 km. In the San-in district, many earthquakes occur at depths of approximately 11 km. At a depth of 11 km, epicenters are located in both areas of high velocity and low velocity (Fig. 4a, c). There are no clear relationships between the locations of earthquakes and the velocity structure in the upper crust beneath the San-in district. In the San-in district, the Moho depth is considered to be 30–35 km (Ueno et al. 2008). At a depth of 25 km, which corresponds to the depth of the lower crust, low-velocity anomalies exist in the lower crust beneath the seismic belt (Fig. 4a, c). The vertical cross-section along line C in Fig. 4c clearly shows that the distribution of low-velocity anomalies in the lower crust corresponds to the distribution of hypocenters in the upper crust.

Discussion

Our result shows that low-velocity zones exist in the lower crust (at a depth of 25 km) beneath the seismic belt in the San-in district (Figs. 4a, 5a). The low-velocity zone beneath the seismic belt is likely to be a weak zone. Our results, therefore, are consistent with the model proposed by Iio et al. (2002). We inferred from our results that in the San-in district, deformation is concentrated in the weak zone in the lower crust by compressive stress that is caused by subductions of the PHS plate and the PAC plate, and stress concentration occurs above the weak zone and is responsible for the formation of the seismic belt there. Nakajima and Hasegawa (2007b) showed that low-velocity anomalies exist in the lower crust beneath the Niigata–Kobe tectonic zone. Their results are consistent with the results we obtained in this study.

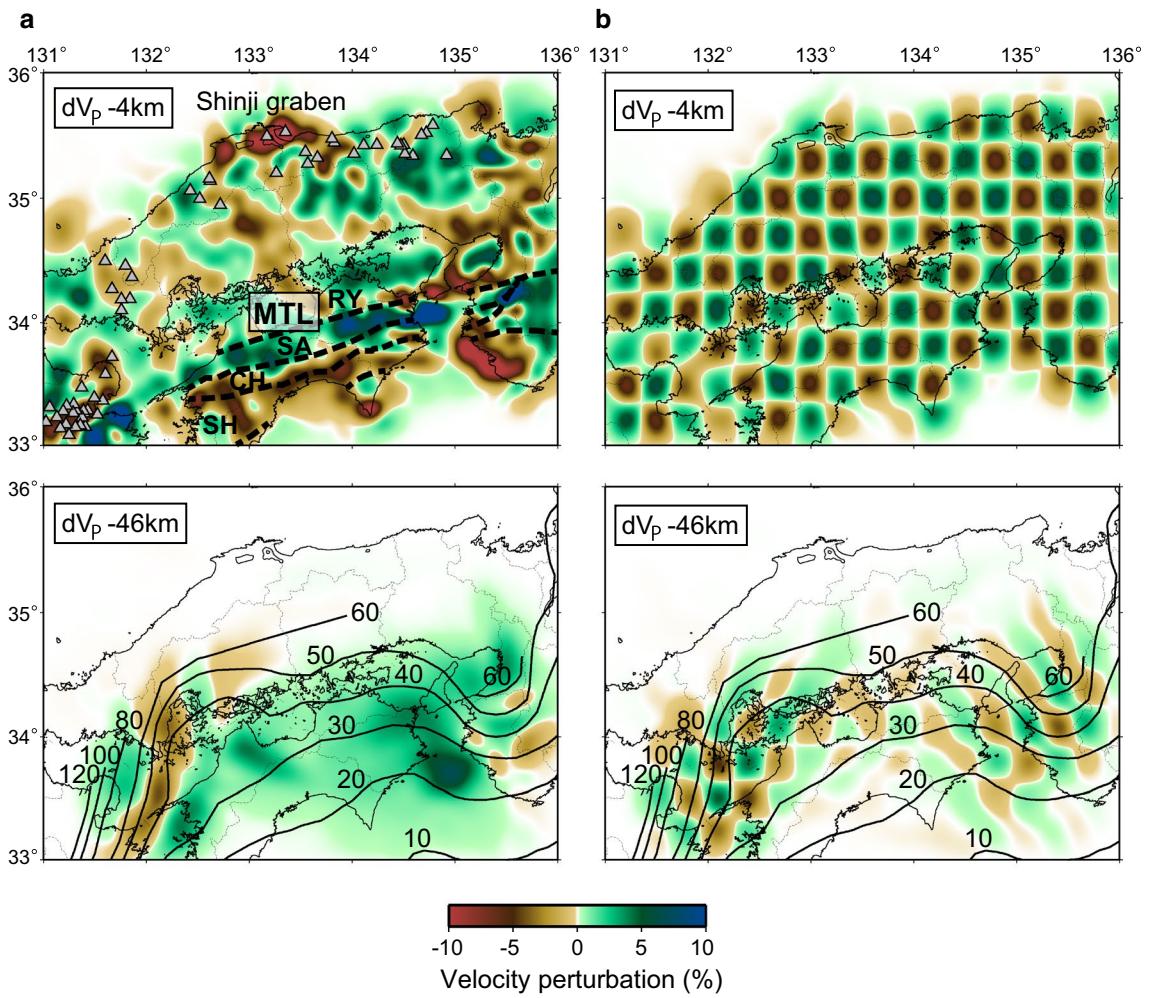

Fig. 3 **a** P-wave velocity perturbations at depths of 4 and 46 km. **b** Results of checkerboard resolution tests at those depths. Velocity perturbations are deviations from the initial velocities at each depth. In the upper panel of **a**, gray triangles denote quaternary volcanoes (Geological Survey of Japan, AIST 2013), and broken lines represent boundaries of geological structures around the MTL (Kodaira et al. 2002). RY, SA, CH, and SH represent the Ryoke belt, Sanbagawa belt, Chichibu belt, and Shimanto belt, respectively. Thick lines in the lower figures represent the isodepth contours of the PHS plate (Baba et al. 2002; Hirose et al. 2008; Nakajima and Hasegawa 2007c)

We next discuss the possible causes of the low-velocity anomalies detected in the lower crust beneath the seismic belt. Two mechanisms can explain the cause of a low-velocity anomaly: high temperature and high water content. We examine whether the temperatures of the low-velocity zones in the lower crust beneath the seismic belt are high.

Cutoff depth of intraplate earthquakes

It is thought that the cutoff depth of shallow earthquakes depends on temperature and that the temperature at a cutoff depth is approximately 300 °C (e.g., Ito 1990). Using this criterion, we can estimate the temperature in the lower crust (at a depth of 25 km) from the cutoff depth of intraplate earthquakes. We used D90, the depth above which 90% of earthquakes occur, as the cutoff depth for intraplate earthquakes. We can consider that the temperature of the lower crust decreases as D90 increases. We calculated the distribution of D90 in the study area and examined the temperature in the lower crust (at a depth of 25 km) beneath the seismic belt.

We calculated D90 using the procedure, which is a simplification of that described by Omuralieva et al. (2012), who calculated the D90 for areas in and around Japan. We used hypocenters determined by the JMA for the calculation. Although these hypocenters were determined without considering 3-D velocity structures, they are useful for obtaining an approximate

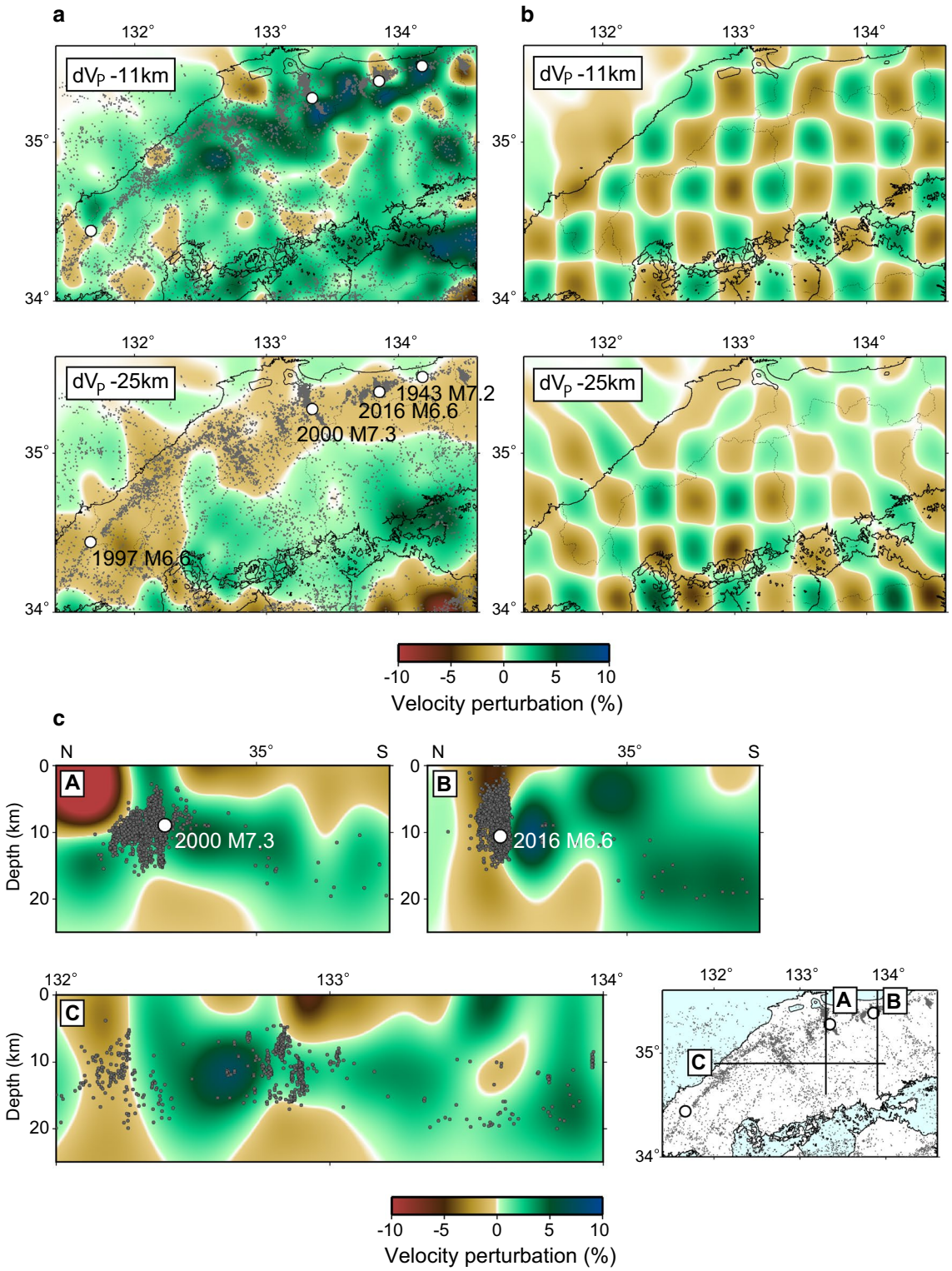

Fig. 4 **a** P-wave velocity perturbations at depths of 11 and 25 km. **b** Results of checkerboard resolution tests at those depths. **c** Vertical cross-sections along lines A–C drawn in the bottom right map. Velocity perturbations are deviations from the initial velocities at each depth. In **a** and **c**, gray dots denote earthquakes of $M_J \geq 1.0$ and depths ≤ 20 km that occurred between January 2001 and December 2016. White circles denote large intraplate earthquakes of $M_J \geq 6.5$ that occurred over the past 100 years

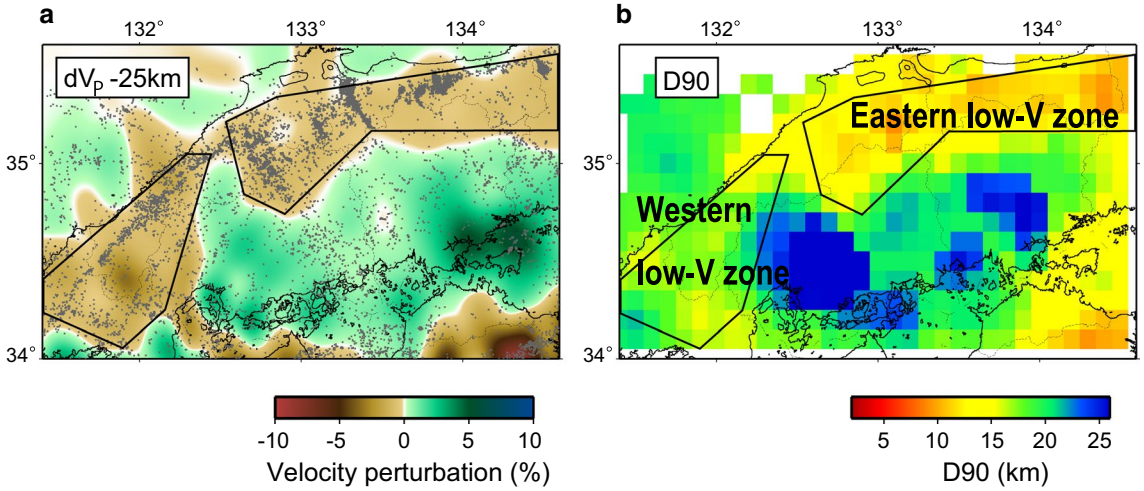

Fig. 5 **a** P-wave velocity perturbations at a depth of 25 km. Velocity perturbations are deviations from the initial velocity. Gray dots denote epicenters of intraplate earthquakes of $M_J \geq 1.0$ and depths ≤ 20 km that occurred between January 2001 and December 2016. **b** Distribution of D90. Colors represent the depth of the D90

estimate of the temperature in the lower crust, because both P- and S-wave arrival times were used. The details of the procedure for calculating D90 are described in Additional file 1.

Figure 5b shows the result of the calculation of the spatial distribution of D90. In the eastern part of the low-velocity zone in the lower crust (at a depth of 25 km) beneath the seismic belt, the D90 is shallow (approximately 10–15 km), while in the western part, the D90 is deeper (approximately 15–20 km) (Fig. 5). Hereinafter, we divide the low-velocity zone in the lower crust beneath the seismic belt into two parts, the eastern part and the western part, which we refer to as the "Eastern low-V zone" and "Western low-V zone", respectively, for convenience (Fig. 5). Temperatures in the Eastern and Western low-V zones are likely to be higher and lower, respectively, because the D90 is shallow and deeper, respectively, in these zones, but there is no clear difference between the number of quaternary volcanoes in these zones (Figs. 3a, 5). On the other hand, D90 in the high-velocity zone in the lower crust south of the seismic belt is very deep (deeper than 20 km) (Fig. 5), and hence, the temperature is likely to be low, and there are no quaternary volcanoes (Figs. 3a, 5). Tanaka et al. (2004) estimated the distribution of heat flows in and around Japan and showed that the heat flows in the Eastern and Western low-V zones are high and low, respectively. Their findings are consistent with our interpretation. Furthermore, the shape of the Eastern low-V zone is very similar to that of a shallow D90 region. Therefore, in the Eastern low-V zone, the main cause of the low-velocity anomaly is likely to be high temperature, while in the Western low-V zone, the main cause of the low-velocity anomaly is likely to be something else.

Cause of high temperature in the eastern low-V zone

Nakajima and Hasegawa (2007a) performed a seismic travel-time tomography of a study area larger than ours and found a low-velocity anomaly that ranged in location from immediately above the PAC plate to near the Moho discontinuity, immediately below the Eastern low-V zone. They concluded that the low-velocity anomaly corresponded to a hot mantle upwelling. Based on this interpretation, we inferred that the temperature of the Eastern low-V zone is high because of the existence of the hot mantle upwelling, and that the resulting high temperature is the main cause of the low-velocity anomaly in the Eastern low-V zone.

Cause of low-velocity anomaly in the Western low-V zone

It is inferred that the temperature of the Western low-V zone is not high unlike the Eastern low-V zone. Nevertheless, the seismic velocity in the Western low-V zone is low. Although we based our inference about the reasons for the high temperature and low velocity in the Eastern low-V zone on the velocity structure in the mantle (Nakajima and Hasegawa 2007a), it is difficult to estimate the velocity structure in the mantle beneath the Western low-V zone reliably due to the insufficient coverage of seismic rays there. However, there are other clues from which we may infer a possible cause of the low-velocity anomaly of the Western low-V zone. Shelly et al. (2006) examined the velocity structure in and around the PHS plate and

detected a high-V_P/V_S zone above the PHS plate, south of the Western low-V zone. Their interpretation of this was that the high-V_P/V_S zone corresponded to water dehydrated from the PHS plate. Based on this interpretation, we concluded that water may have dehydrated from the PHS plate beneath the Western low-V zone and reached the Western low-V zone. We inferred from this that the main cause of the low-velocity anomaly of the Western low-V zone may be the existence of thus water. Thus, we can explain the temperature of the Western low-V zone not being high and its velocity being low as follows. It is possible that the temperature of the Western low-V zone is not high because a mantle upwelling does not exist beneath the Western low-V zone, unlike beneath the Eastern low-V zone, or if it does exist, it does not extend to near the Western low-V zone because it is blocked by the PHS plate. On the other hand, water dehydrated from the PHS plate reaches the Western low-V zone, and this water may be the cause of the low-velocity anomaly.

Conclusion

Using seismic travel-time tomography, we reveal that a low-velocity zone exists in the lower crust beneath the seismic belt in the San-in district, Japan. We infer that deformation in the San-in district was concentrated in the low-velocity zone, that stress concentration occurred above the low-velocity zone, and that the seismic belt was formed there as a result.

We calculated cutoff depths of intraplate earthquakes that occurred in the San-in district. The results show that the cutoff depths in the eastern part of the low-velocity zone in the lower crust beneath the seismic belt are shallow, while those in the western part are deeper. Hence, the temperature of the eastern part is likely to be high, while that of the western part is likely to be lower. Taking into consideration the results of previous studies together with the results of our study, we conclude that it is likely that the temperature of the eastern part is high because of the presence of the mantle upwelling at shallow depth just below the eastern part and that the main cause of the low-velocity anomaly is the high temperature in this area. On the other hand, the temperature of the western part is not high, although its velocity is low. Thus, we infer it is possible that water dehydrated from the PHS plate reaches the western part and that the main cause of the low-velocity anomaly is the existence of this water.

Supplementary information

Supplementary information accompanies this paper at https://doi.org/10.1186/s40623-019-1091-x.

Additional file 1. Procedure for calculating D90.

Abbreviations

M_J: Japan Meteorological Agency magnitude; PHS: Philippine Sea; PAC: Pacific; JMA: Japan Meteorological Agency; MTL: Median Tectonic Line; V_P: P-wave velocity; CRT: checkerboard resolution test.

Acknowledgements

We used arrival time data reported in the earthquake catalog unified by the JMA. We used GMT (Wessel and Smith 1991) to draw all of the figures. Constructive comments by two anonymous reviewers helped to improve the manuscript.

Authors' contributions

HT carried out the analysis and wrote the manuscript. HT and YI contributed to the interpretations and preparation of the manuscript. TS helped with the analysis. All authors read and approved the final manuscript.

Funding

This study was partly supported by MEXT KAKENHI Grant Number 26109006.

Availability of data and materials

The data used in this study are available at the JMA website (http://www.data.jma.go.jp/svd/eqev/data/bulletin/deck.html, in Japanese).

Ethics approval and consent to participate

Not applicable.

Consent for publication

Not applicable.

Competing interests

The authors declare that they have no competing interests.

Author details

[1] Graduate School of Science, Kyoto University, Kyoto, Japan. [2] Disaster Prevention Research Institute, Kyoto University, Kyoto, Japan.

Received: 3 July 2019 Accepted: 16 October 2019
Published online: 25 October 2019

References

Baba T, Tanioka Y, Cummins PR, Uhira K (2002) The slip distribution of the 1946 Nankai earthquake estimated from tsunami inversion using a new plate model. Phys Earth Planet Inter 132:59–73. https://doi.org/10.1016/S0031-9201(02)00044-4

Christensen NI (1979) Compressional wave velocities in rocks at high temperatures and pressures, critical thermal gradients, and crustal low-velocity zones. J Geophys Res 84:6849–6857. https://doi.org/10.1029/JB084iB12p06849

de Kool M, Rawlinson N, Sambridge M (2006) A practical grid-based method for tracking multiple refraction and reflection phases in three-dimensional heterogeneous media. Geophys J Int 167:253–270. https://doi.org/10.1111/j.1365-246X.2006.03078.x

Geological Survey of Japan, AIST (2013) Volcanoes of Japan. https://gbank.gsj.jp/volcano/index.htm/. Accessed 26 May 2019

Heki K, Miyazaki S, Takahashi H, Kasahara M, Kimata F, Miura S, Vasilenko NF, Ivashchenko A, An K (1999) The Amurian Plate motion and current plate kinematics in eastern Asia. J Geophys Res 104:29147–29155. https://doi.org/10.1029/1999JB900295

Hirose F, Nakajima J, Hasegawa A (2008) Three-dimensional seismic velocity structure and configuration of the Philippine Sea slab in southwestern Japan estimated by double-difference tomography. J Geophys Res 113:B09315. https://doi.org/10.1029/2007JB005274

Iio Y, Sagiya T, Kobayashi Y, Shiozaki I (2002) Water-weakened lower crust and its role in the concentrated deformation in the Japanese Islands. Earth Planet Sci Lett 203:245–253. https://doi.org/10.1016/S0012-821X(02)00879-8

Ito K (1990) Regional variations of the cutoff depth of seismicity in the crust and their relation to heat flow and large inland-earthquakes. J Phys Earth 38:223–250. https://doi.org/10.4294/jpe1952.38.223

Kawanishi R, Iio Y, Yukutake Y, Shibutani T, Katao H (2009) Local stress concentration in the seismic belt along the Japan Sea coast inferred from precise focal mechanisms: implications for the stress accumulation process on intraplate earthquake faults. J Geophys Res 114:B01309. https://doi.org/10.1029/2008JB005765

Kodaira S, Kurashimo E, Park JO, Takahashi N, Nakanishi A, Miura S, Iwasaki T, Hirata N, Ito K, Kaneda Y (2002) Structural factors controlling the rupture process of a megathrust earthquake at the Nankai trough seismogenic zone. Geophys J Int 149:815–835. https://doi.org/10.1046/j.1365-246X.2002.01691.x

Kohlstedt DL, Evans B, Mackwell SJ (1995) Strength of the lithosphere: constraints imposed by laboratory experiments. J Geophys Res 100:17587–17602. https://doi.org/10.1029/95JB01460

Nakajima J, Hasegawa A (2007a) Tomographic evidence for the mantle upwelling beneath southwestern Japan and its implications for arc magmatism. Earth Planet Sci Lett 254:90–105. https://doi.org/10.1016/j.epsl.2006.11.024

Nakajima J, Hasegawa A (2007b) Deep crustal structure along the Niigata-Kobe Tectonic Zone, Japan: its origin and segmentation. Earth Planets Space 59:e5–e8. https://doi.org/10.1186/BF03352677

Nakajima J, Hasegawa A (2007c) Subduction of the Philippine Sea plate beneath southwestern Japan: slab geometry and its relationship to arc magmatism. J Geophys Res 112:B08306. https://doi.org/10.1029/2006JB004770

Nakao S, Shibutani T, Nishida R, Tsukuda T, Oike K (1991) Relation between seismic gaps and occurrence of earthquakes in active seismic zones. Annu Disas Prev Res Inst Kyoto Univ 34(B-1):231–251 **(in Japanese with English abstract)**

Nishimura T, Takada Y (2017) San-in shear zone in southwest Japan, revealed by GNSS observations. Earth Planets Space 69:85. https://doi.org/10.1186/s40623-017-0673-8

O'Connell RJ, Budiansky B (1974) Seismic velocities in dry and saturated cracked solids. J Geophys Res 79:5412–5426. https://doi.org/10.1029/JB079i035p05412

Omuralieva AM, Hasegawa A, Matsuzawa T, Nakajima J, Okada T (2012) Lateral variation of the cutoff depth of shallow earthquakes beneath the Japan Islands and its implications for seismogenesis. Tectonophysics 518–521:93–105. https://doi.org/10.1016/j.tecto.2011.11.013

Rawlinson N, de Kool M, Sambridge M (2006) Seismic wavefront tracking in 3D heterogeneous media: applications with multiple data classes. Explor Geophys 37:322–330. https://doi.org/10.1071/EG06322

Shelly DR, Beroza GC, Ide S, Nakamura S (2006) Low-frequency earthquakes in Shikoku, Japan, and their relationship to episodic tremor and slip. Nature 442:188–191. https://doi.org/10.1038/nature04931

Shibutani T, Katao H, Group for the dense aftershock observations of the 2000 Western Tottori Earthquake (2005) High resolution 3-D velocity structure in the source region of the 2000 Western Tottori Earthquake in southwestern Honshu, Japan using very dense aftershock observations. Earth Planets Space 57:825–838. https://doi.org/10.1186/BF03351861

Tanaka A, Yamano M, Yano Y, Sasada M (2004) Geothermal gradient and heat flow data in and around Japan (I): appraisal of heat flow from geothermal gradient data. Earth Planets Space 56:1191–1194. https://doi.org/10.1186/BF03353339

Ueno H, Hatakeyama S, Aketagawa T, Funasaki J, Hamada N (2002) Improvement of hypocenter determination procedures in the Japan Meteorological Agency. Q J Seismol 65:123–134 **(in Japanese with English abstract)**

Ueno T, Shibutani T, Ito K (2008) Configuration of the continental Moho and Philippine Sea slab in southwest Japan derived from receiver function analysis: relation to subcrustal earthquakes. Bull Seismol Soc Am 98(5):2416–2427. https://doi.org/10.1785/0120080016

Wessel P, Smith WHF (1991) Free software helps map and display data. EOS Trans AGU 72:441–446. https://doi.org/10.1029/90EO00319

Zhao D, Tani H, Mishra OP (2004) Crustal heterogeneity in the 2000 western Tottori earthquake region: effect of fluids from slab dehydration. Phys Earth Planet Inter 145:161–177. https://doi.org/10.1016/j.pepi.2004.03.009

Zhao D, Liu X, Hua Y (2018) Tottori earthquakes and Daisen volcano: effects of fluids, slab melting and hot mantle upwelling. Earth Planet Sci Lett 485:121–129. https://doi.org/10.1016/j.epsl.2017.12.040

Publisher's Note